Conf-910505--54

Fabrication and Tests of Prototype Quadrupole Magnets for the Storage Ring of the Advanced Photon Source*

S. H. Kim, K. M. Thompson, E. L. Black and J. M. Jagger
Argonne National Laboratory
Argonne, IL 60439 USA

ANL/CP--73048

DE91 012001

Abstract

Prototype quadrupole magnets for the APS storage ring have been fabricated and tested. Mechanical stability of the magnet poles and acceptable field quality have been achieved. Geometries of the pole-end bevels have been studied in order to simplify the design of the magnet end-plate.The field saturation at different segments of the magnet has been measured to evaluate the magnet efficiency.

I. INTRODUCTION

The magnetic lattice of the positron storage ring for the 7-Gev Advanced Photon Source (APS) requires 400 quadrupole magnets [1]. The quadrupoles are of the conventional resistive type, and have three different magnetic lengths and five families as shown in Table 1. The required beam stay-clear aperture is x=±35 mm and y=±20 mm. Each magnet is excited by an independent power supply. The design of the magnets is the same except for the length of the magnet.

Figure 1 shows the current-lead end of the 0.8-m length prototype quadrupole with a section of the vacuum chamber for the positron beam. The magnet design is restricted by the requirements of the vacuum chamber geometry for the photon beam ports and antechamber. Consequently, the magnet does not have the flux return yoke between the top and bottom halves of the magnet, and has relatively long narrow magnet poles [2-3]. Two prototype magnets have been fabricated and tested using the rotating coil method.

The normal and skew multipole field coefficients, b_n and a_n, for a 2-D magnetic field, $B = B_y + i B_x$, are defined

$$B = Bo \sum_{n=0}^{\infty} (b_n + a_n) (x + i y)^n \qquad (1)$$

where the coefficients are in cm^{-n} units, and b_1=1.0 cm^{-1} and a_1=0 for a normal quadrupole magnet. Relative values of the coefficients with respect to the main quadrupole field component at radius r_o=2.5 cm are used:

$$b_n(\text{at } r_o) = b_n r_o^n / b_1 r_o,\ a_n(\text{at } r_o) = a_n r_o^n / b_1 r_o. \qquad (2)$$

II. MAGNET DESIGN AND FABRICATION

Figure 2 shows the end-view of a one-half section of the magnet. The magnet pole has 45° symmetry and is tapered to reduce the flux saturation. In order to minimize the physical length of the magnet for a given length of the core, which is 0.765m long, the magnet end-plate has chamfers of 19.1-mm/45°-cut as shown in Fig. 2 so that the magnet coil fits snugly to the magnet pole.

Table I
Parameters of the storage ring quadrupole magnets for the 7-Gev operation.

	Q1	Q2	Q3	Q4	Q5
L (m)	0.50	0.80	0.50	0.50	0.60
B' (T/m)	-10.843	15.792	-10.585	-18.902	18.248
B'L (T)	-5.421	12.634	-5.293	-9.451	10.949
I (A)[a]	215	320	210	415	390
ε (%)[a]	99	97.5	99	89	92

[a] Measured data from the prototype magnets.

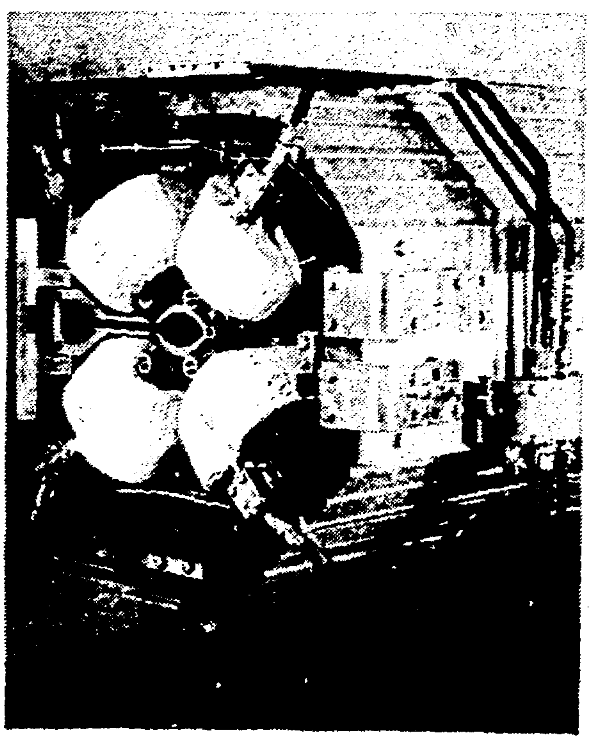

Fig. 1. Photograph of the current-lead end of the 0.8-m prototype quadrupole magnet.

* Work supported by the U.S. Department of Energy, Office of Basic Energy Sciences, under Contract No. W-31-109-ENG-38

DISCLAIMER

The end plate is designed to have a removable pole-tip. The removable pole-tip does not have the 45°-cut chamfers. This requires the attachment of the pole-tips after the installation of the magnet coils.

The two quadrants of the assembled laminations are welded at weld joints "A" and "B" as shown in Fig. 2 The weld joints have welding-relief grooves to reduce the effects of weld *shrinkage. The laminations are* 1.52-mm thick low carbon steel. The laminations have alignment notches as shown in Fig. 2 in order to install a removable alignment fixture for the measurements of the magnetic center axis. The alignment fixture is eventually to be used for the survey of the storage ring.

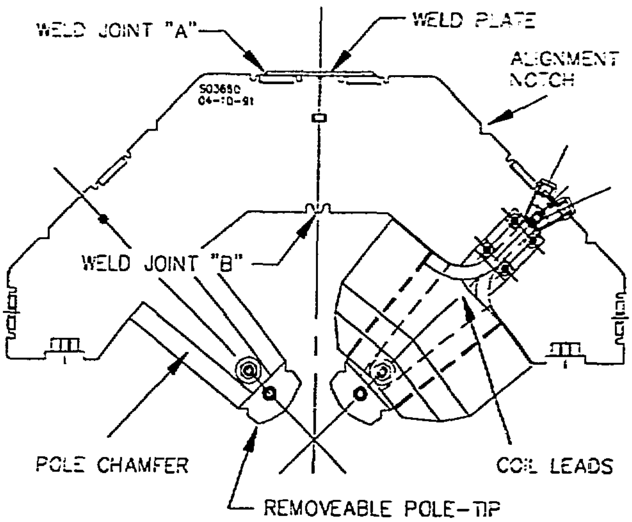

Fig.2. End-view of the top-half section of the magnet.

III. MAGNET MEASUREMENTS

A. Mechanical Stability

For the first prototype magnet the two quadrants were welded only at weld joint "A" in Fig. 2. That left a gap at "B", due to which magnet pole movements of approximately 0.15 mm at high field were observed. Additional welds at "B" between the two quadrants for both prototype magnets prevented any pole movements and achieved the mechanical stability of the magnets.

The magnet pole movements before and after the additional welds were reflected in the skew sextupole and normal octapole field coefficients.

B. Multipole Field Coefficients

Shown in Fig. 3 are the normal and skew multipole field coefficients for the second prototype magnet at a beam aperture radius of 2.5 cm.The magnet excitation currents listed in Table 1 for the five families of the quadrupoles are within the measurement currents in Fig. 3.

After the main quadrupole field component, the first two allowable terms are b_5 (duodecapole) and b_9 (20-pole) and the corresponding skew coefficients. The values of the two coefficients are obtained with a pole end-bevel geometry of 12.8 mm x 12.8 mm-cut. Two-dimensional calculations of the two coefficients at a high excitation current are $b_5=-0.34\times10^{-4}$ and $b_9=0.69\times10^{-4}$. The "body" measurements of the two coefficients agree with calculations within 1×10^{-4}.

In Fig. 3 the two largest unallowed coefficients are sextupole and octapole terms, $b_2=2.5\times10^{-4}$ and $b_3=3.5\times10^{-4}$. They are due to the imperfections in the stacking of the laminations, welding of the two quadrants and assembly of the top and bottom half-magnet. All these multipole coefficients are within acceptable levels for the dynamic aperture of the positron beam in the storage ring.

C. Pole-End Bevels

The pole-end bevels in the removable pole-tips for the reference design have a geometry of 12.8 mm x 12.8 mm-cut. The bevels increased b_5 by 5.5×10^{-4} and reduced b_9 by 0.1×10^{-4} compared to those two allowable terms for the pole-tips without any bevels.

In Table 2, the changes of b_5 and b_9 for five different pole-bevels and corner-cuts are listed. It shows that b_9 is relatively insensitive to the bevel geometry and corner-cut compared to b_5. For the bevels 9.6 mm x 17.4 mm with a corner-cut up to 16.5 mm, the coefficients are within 2×10^{-4} units.

Table 2
Pole-end bevels on the removable pole-tips and integrated b_5 and b_9 coefficients at 2.5 cm in 10^{-4}unit for the 0.8-m prototype at two excitation currents.

	250.7 A		450.6 A	
Pole-end bevels (mm)	b_5	b_9	b_5	b_9
a. 12.8x12.8	0.19	-0.53	-1.14	-0.59
b. 9.6x17.4	2.67	-0.62	1.13	-0.68
c. 9.6x17.4 with 12.8 corner-cut[a]	0.09	-0.74	-1.09	-0.78
d. 9.6x17.4 with 16.5 corner-cut	-0.64	-0.80	-2.01	-0.83
e. 9.6x17.4 with 19.1 corner-cut	-1.42	-0.83	-3.88	-0.88

[a] Corner-cuts are in the same direction with the chamfers of the magnet end-plates.

D. Excitation Efficiency

Plotted in Fig. 4 are the measured data of the field gradient integrals normalized to the excitation currents. The gradient integrals of the two prototypes differed by less than 5×10^{-3} for the currents higher than 250 A.

Normalized field gradients, B'/I, for different segments of the magnet were measured at two currents and listed in Table 3. For the permeability of the lamination $\mu=\infty$, the calculated gradient is $B'/I=5.18363\times10^{-2}$ T/m·A. Two-dimensional calculation of the efficiency of the excitation at 450A (7.3Gev) is 88.5% compared to the measured data of 87.2%.

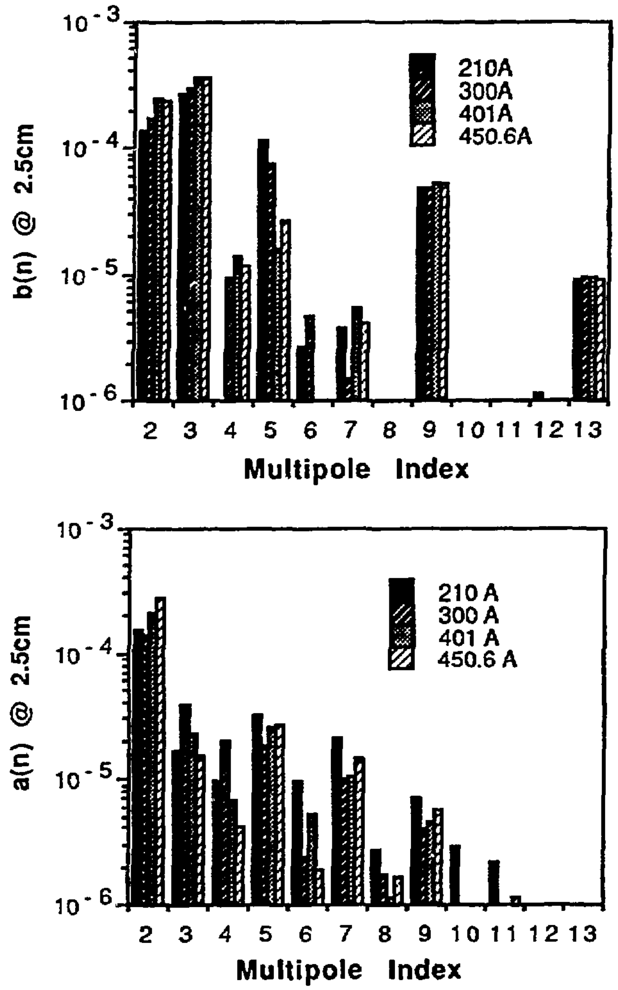

Fig. 3. Magnitude of the relative multipole field coefficients at r_0=2.5 cm. The following coefficients have negative values: b_5 at 450.6A, b_6, b_9, b_{13}, a_3, a_4 except at 210A, a_6, a_8 at 410A and 450.6A, a_9 at 450.6A, and a_{10}.

IV. Conclusion

From the fabrication and measurements of two prototype quadrupoles for the storage ring, mechanical stability of the magnet poles, a routine assembly procedure for the fabrication of production magnets and acceptable field quality in terms of multipole coefficients have been achieved. Use of removable pole-tip geometries of pole-end bevels has been investigated in order to design the magnet end-plate. A higher excitation efficiency for the operation above 7-Gev is desirable.

Table 3
Field gradients at different sections in the longitudinal direction normalized to the magnet excitation currents

	B'/I (10^{-2} T/m·A)	
z (m)	at 250.79A	at 450.75A
0 - 0.215	5.122	4.518
0.215 - 0.270	5.101	4.485
0.270 - 0.325	4.499	4.208

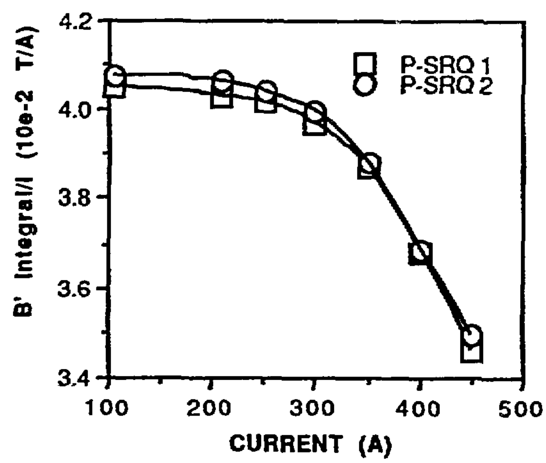

Fig. 4. Magnet excitations of the two prototype quadrupoles.

V. Acknowledgments

The authors are grateful to P. Mazur and B. Brown for the initial tests of the magnet at Fermilab. Helpful suggestions and discussions with F. Mills are greatly appreciated.

VI. References

[1] "7-Gev Advanced Photon Source," Conceptual Design Report, Argonne National Laboratory, ANL-87-15, 1987.

[2] K. M. Thompson, S. H. Kim, R. J. Lari and L. R. Turner, "Quadrupole Magnet for the APS Storage Ring," *Proceedings of the 1989 IEEE Particle Accelerator Conference*, Chicago, March 1989, pp. 396-398.

[3] L. R. Turner, S. H. Kim and K. M. Thompson, "Computation of a Quadrupole Magnet for the APS Storage Ring," in press in the IEEE Trans. in Magnetics.